Supporting Information

Novel Near-Infrared II Aggregation-Induced Emission Dots for *In Vivo* Bioimaging

Jiacheng Lin,[a,b†] Xiaodong Zeng,[a,b†] Yuling Xiao,[a,b†] Lin Tang,[a] Jinxia Nong,[a] Yufang Liu,[a] Hui Zhou,[a,b] Bingbing Ding,[a] Fuchun Xu,[c] Hanxing Tong,[d] Zixin Deng[a] and Xuechuan Hong*[a,b,c]

[a]State Key Laboratory of Virology, Key Laboratory of Combinatorial Biosynthesis and Drug Discovery (MOE), Hubei Provincial Key Laboratory of Developmentally Originated Disease, Wuhan University School of Pharmaceutical Sciences, Wuhan 430071, China.

*E-mail: xhy78@whu.edu.cn

[b]Shenzhen Institute of Wuhan University, Shenzhen, 518057, China

[c]Innovation Center for Traditional Tibetan Medicine Modernization and Quality Control, Medical College, Tibet University, Lhasa, 850000, China

[d]Department of General Surgery, Zhongshan Hospital, Fudan University, Shanghai, 200032, China

† These authors contributed equally to this work.

Author contributions

X. C. Hong conceived and designed the experiments. J. C. Lin, X. D. Zeng, Y. L. Xiao, L. Tang, J. X. Nong, Y. F. Liu performed the experiments. H. Zhou, B. B. Ding, F. C. Xu, H. X. Tong, Z. X. Deng, X. C. Hong analyzed the data and wrote the manuscript. All authors discussed the results and commented on the manuscript.

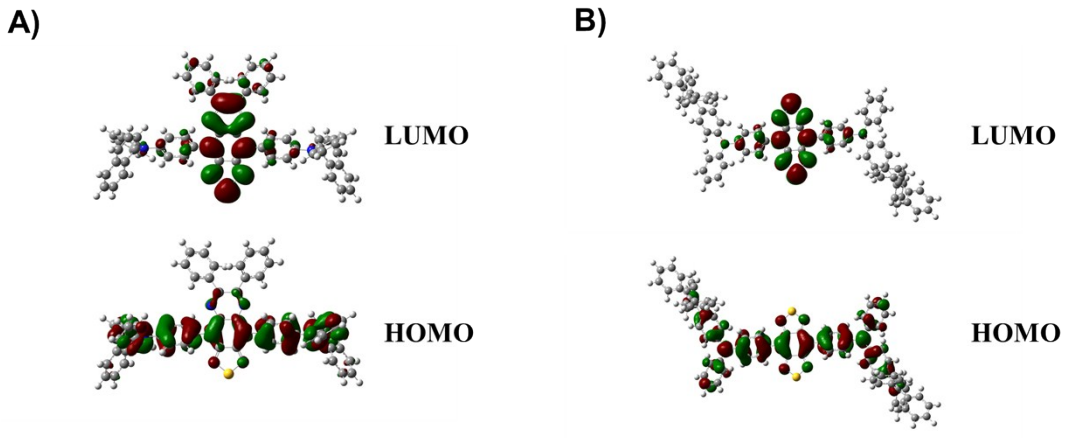

C)

Dye	LUMO [eV]	HOMO [eV]	Egap [eV]	λ_{abs} [nm]	λ_{ex} [nm]	Stokes shift [nm]
TQ-BPN	-3.04	-4.98	1.94	611[a]	811[a]	200
TB1	-3.30	-4.80	1.50	740[b]	975[b]	235
HLZ-BTED	-3.35	-4.50	1.15	805[c]	1034[c]	229

Data measured in (a) Dichloromethane, (b) Tetrahydrofuran, (c) Water, in DSPE-mPEG nanoparticles.

Figure S1. HOMO and LUMO orbital surfaces of **TQ-BPN** (A) and **TB1** (B) in the geometrically optimized structure using the B3LYP/6-31G(d,p) scrf = (cpcm, solvent =CH_2Cl_2) in Gaussian 09 program[1]; (C) Comparison of **HLZ-BTED** with reported SWIR AIE dye **TQ-BPN** and **TB1**. *E*gap (energy gap) = LUMO-HOMO.

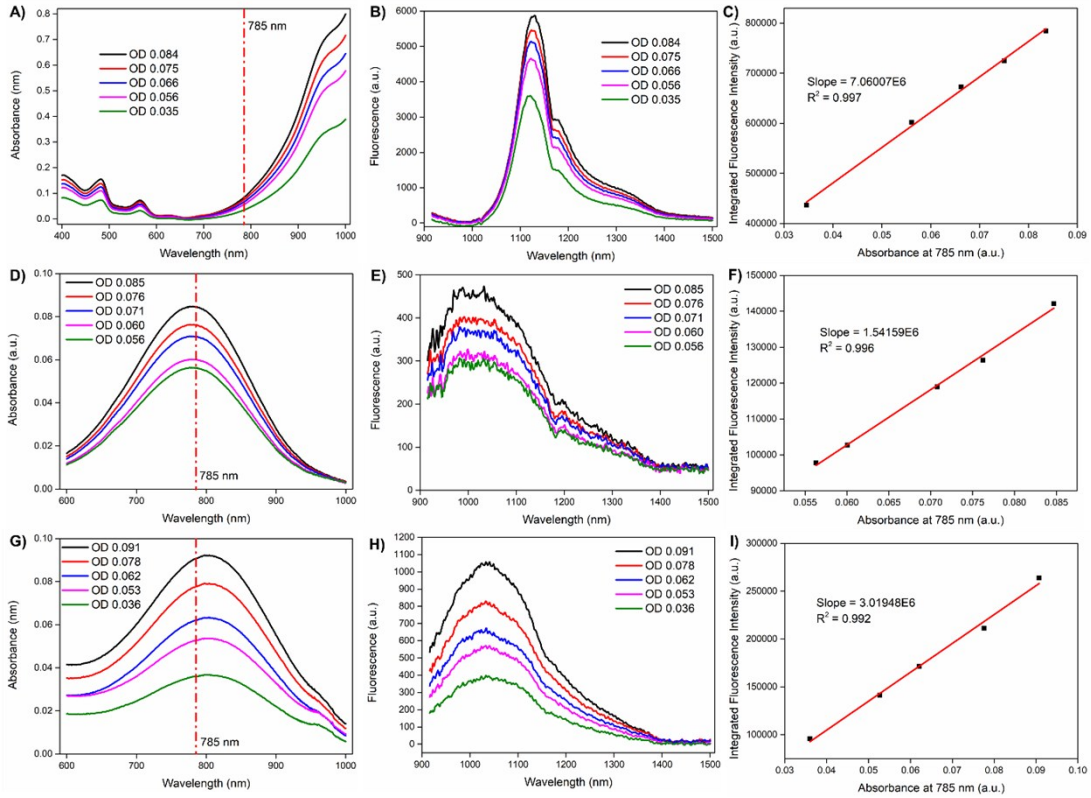

Figure S2. Fluorescence quantum yield measurements of **HLZ-BTED** in THF and its dots in water. Absorbance (A, D, G) and fluorescence (B, E, H) spectra of IR-26 in DCE (A, B), **HLZ-BTED** in THF (D, E), and **HLZ-BTED** dots in water (G, H). The integrated fluorescence was plotted against absorbance for both IR26 and fluorophores and fitted into a linear function, linear fit of IR-26 (C), **HLZ-BTED** (F), and **HLZ-BTED** dots(I). The quantum yield was calculated in the following manner:

$$QY_{sample} = QY_{IR26} \times \frac{Slope_{\ sample}}{Slope_{\ IR26}} \times \frac{{n_{sample}}^{\ 2}}{{n_{IR26}}^{2}}$$

Where QY_{sample} is the QY of fluorophore **HLZ-BTED** in THF or **HLZ-BTED** dots in water, QY_{IR26} is the QY of IR-26 in DCE, n_{sample} and n_{IR26} are the refractive indices of corresponding solvents and DCE.

A)

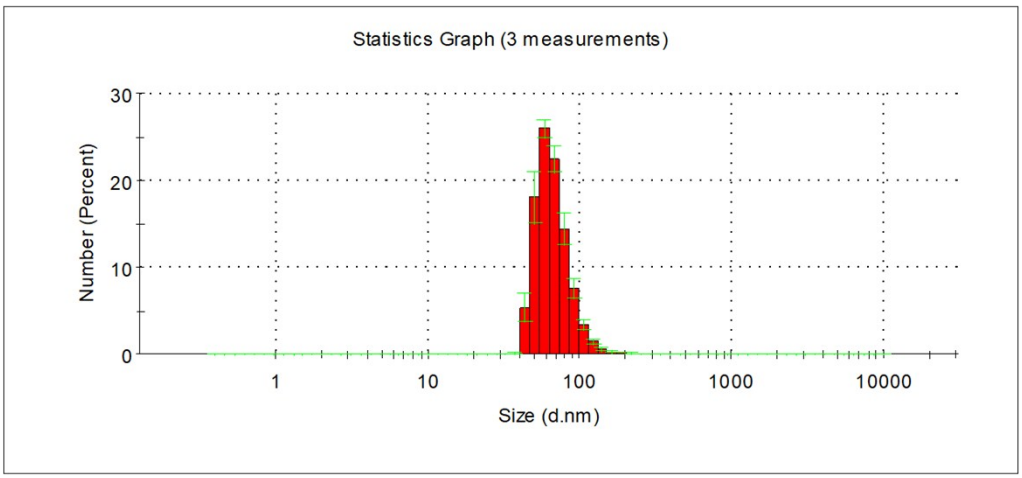

B)

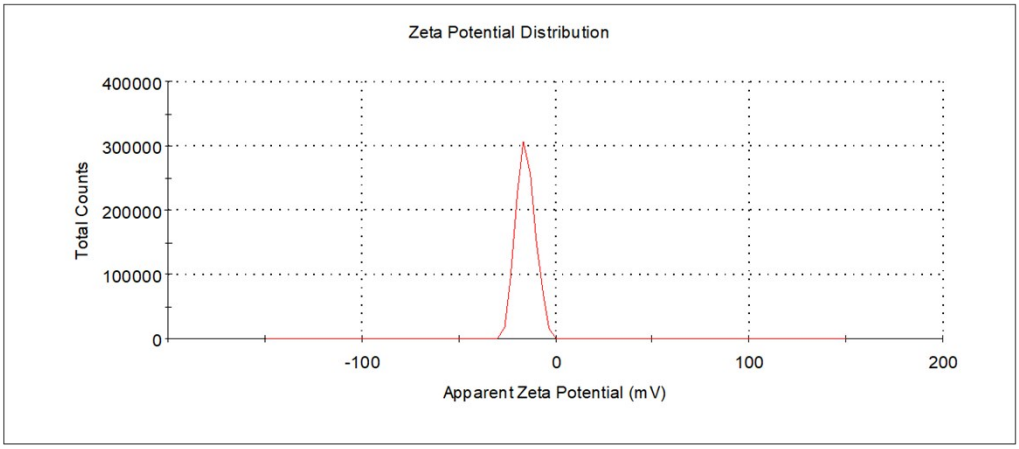

Figure S3. (A) The size distribution of **HLZ-BTED** dots in water based on dynamic light scattering (DLS) measurement (3 measurements, hydrodynamic size ~60 nm). (B) Zeta potential (-16.3 mV) of **HLZ-BTED** dots in water.

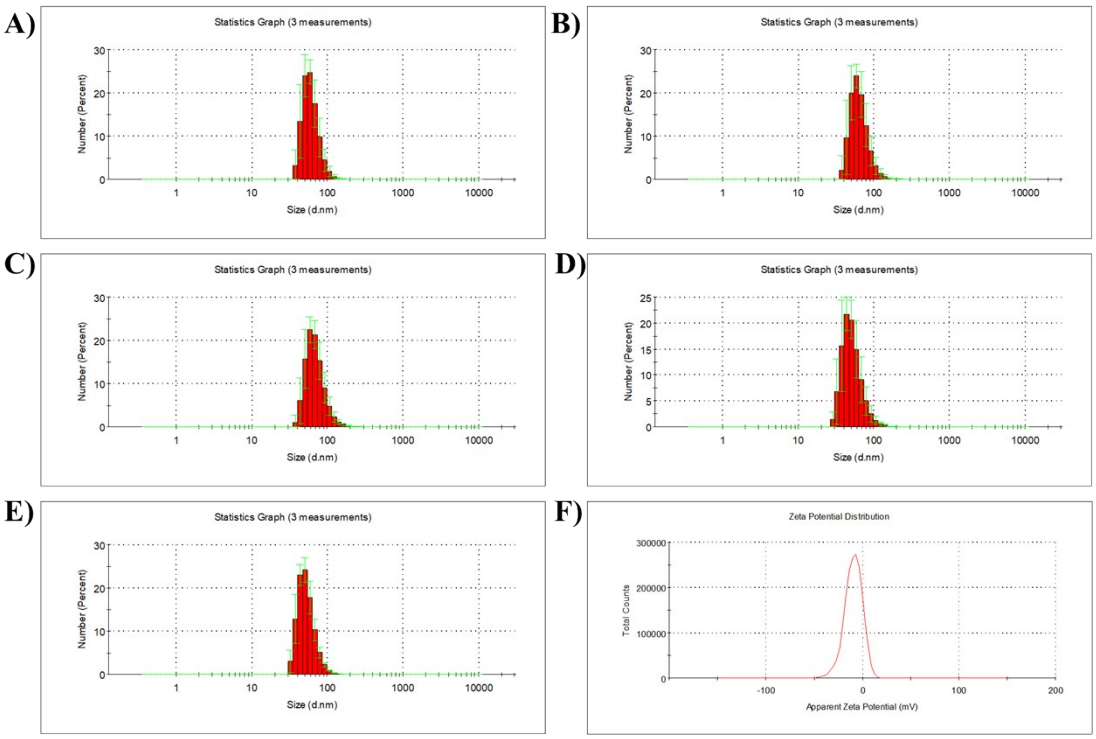

Figure S4. The stability evaluation of **HLZ-BTED** dots in physiological media based on hydrodynamic size (A-E) and zeta potential (F) measurements. **HLZ-BTED** dots were incubated in 5% FBS in PBS at different time points. The hydrodynamic size (~60 nm) at 0 hour (A), 3 hours (B), 6 hours (C), 9 hours (D), and 24 hours (E), had no obvious changes compared with aqueous media, and the zeta potential (F) incubated in physiological media for 24 hours showed a negative value (-9.28 mV).

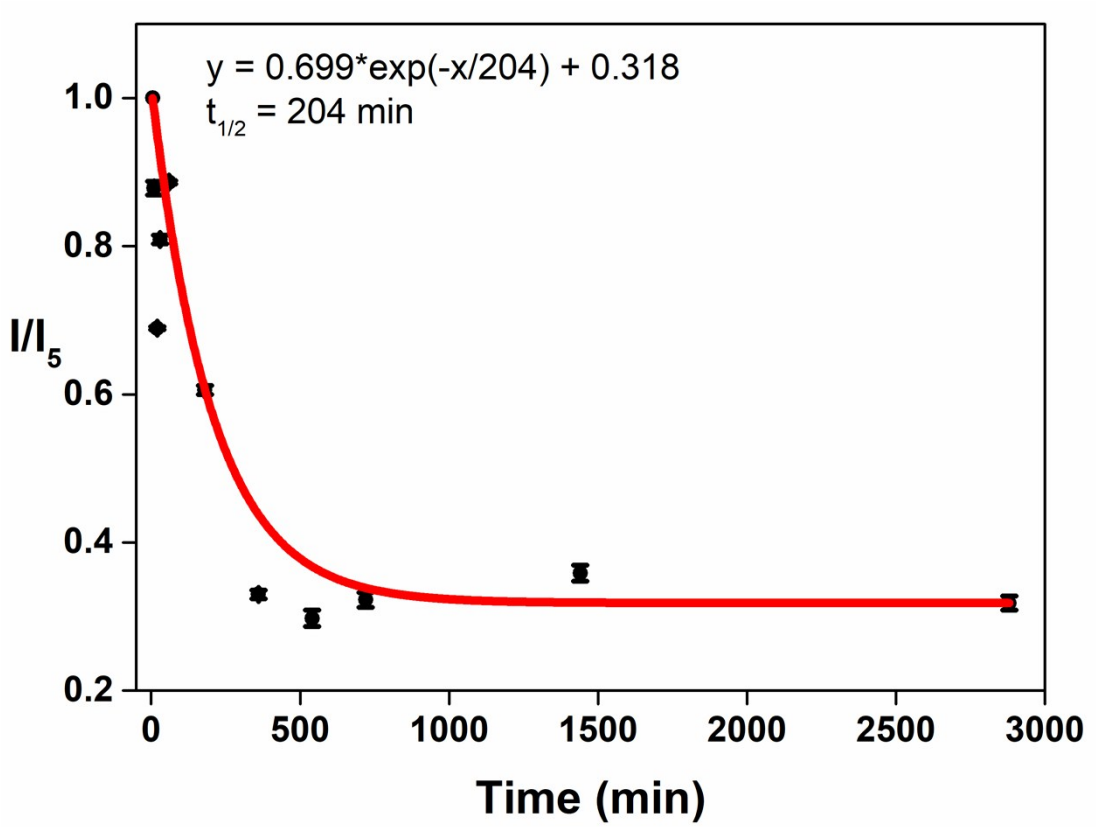

Figure S5. Blood circulation half-life curve of **HLZ-BTED** dots in mice. The circulation half-life was determined to be 204 minutes by fitting the data (5, 10, 20, 30, 60, 180, 360, 540, 720, 1,440, 2,880 min) to a first-order exponential decay (n = 3).

A)

BSA Conc. (nM)	Response	K_D (nM)	kass(1/Ms)	kdiss(1/s)	Full R^2
1000	0.8231	0.0303	1.13E+04	3.44E-07	0.990272
100	0.2104	0.0303	1.13E+04	3.44E-07	0.990272
10	0.0215	0.0303	1.13E+04	3.44E-07	0.990272

B)

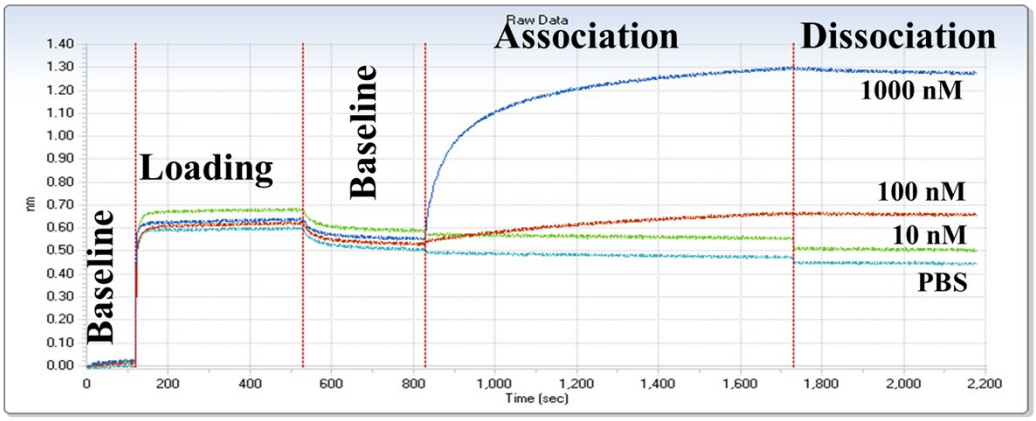

Figure S6. (A) Kinetic binding assay results of **HLZ-BTED** dots to bovine serum albumin measured by bio-layer interferometry (BLI). (B) Sensorgram of the test performance. The binding kinetics of **HLZ-BTED** dots to BSA were evaluated on an Octet Red96 instrument (ForteBio, Inc.) as well as a blank sample containing PBS buffer for the reference. **HLZ-BTED** dots were loaded onto aminopropylsilane (APS) biosensors and the rpm setting for all step was 1000 rpm. The test temperature was 30 ^{o}C. Data processing was performed using Octet Analysis software 7.0 provided by the manufacturer.

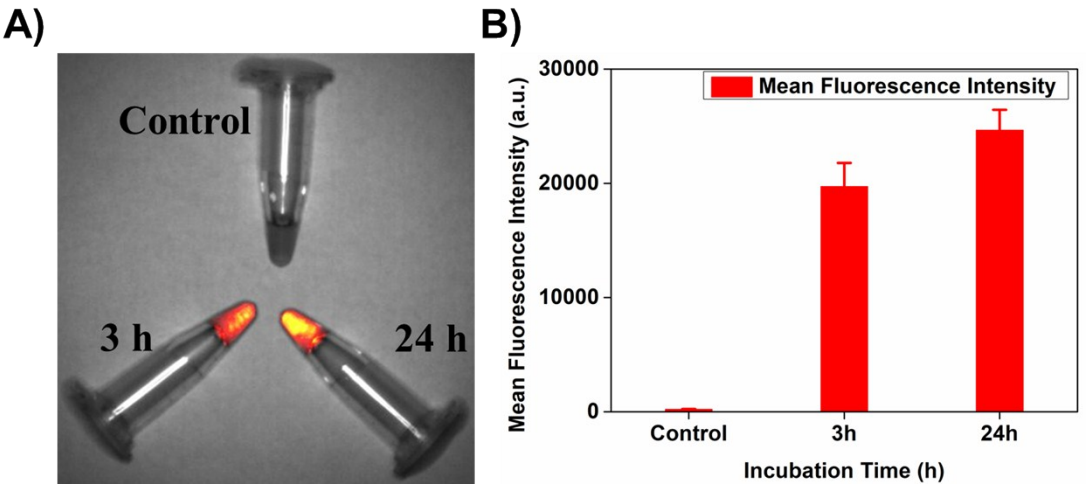

Figure S7. (A) Representative *in vitro* cellular uptake image (90 mW cm^{-2} 808 nm excitation, 1000 nm LP and 10 ms) of 4T1 cells incubated with **HLZ-BTED** dots (100 μg/mL) for 3 hours and 24 hours, blank 4T1 cells as the control. (B) The quantitative analysis of mean fluorescence intensity of 4T1 cells at different incubation time (n = 3).

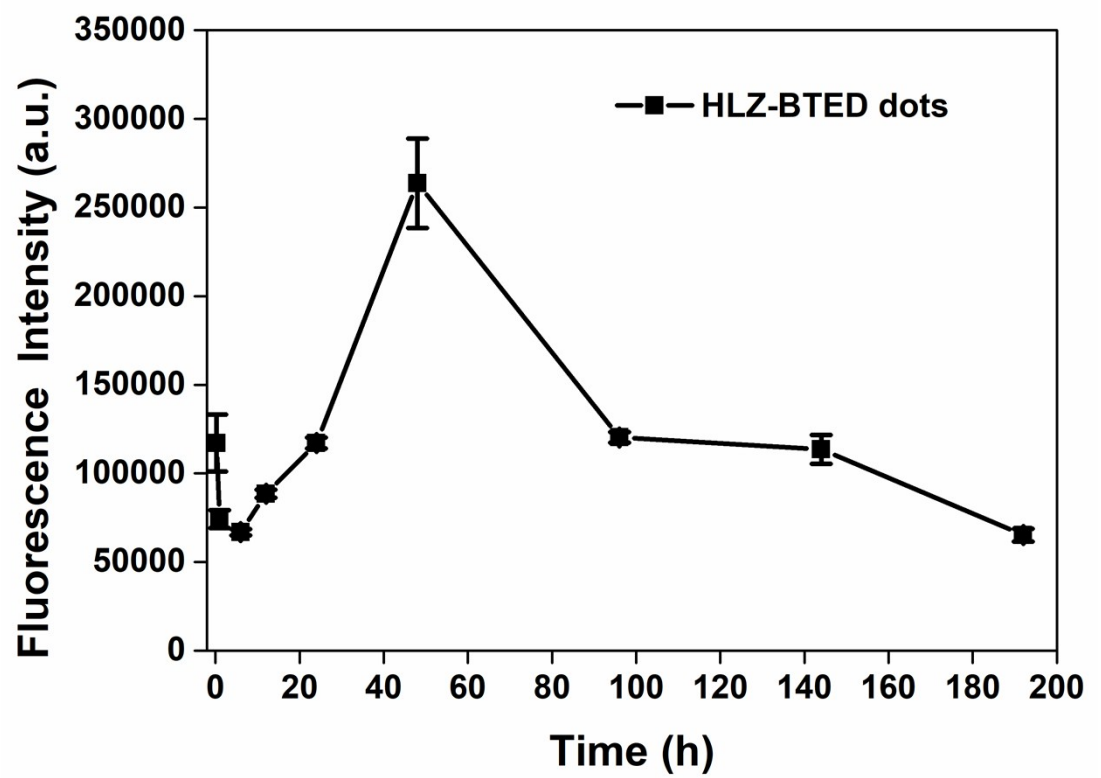

Figure S8. The quantitative analysis of fluorescence intensity of 4T1 mammary tumor mice at different time points after tail vein injection of **HLZ-BTED** dots (0.2 mL, 10 mg kg^{-1}).

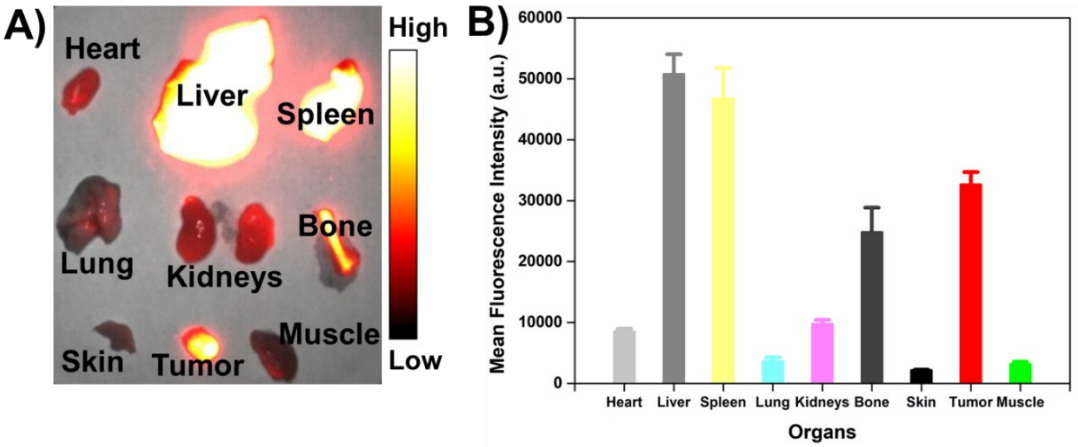

Figure S9. (A) The *ex vivo* biodistribution analysis of **HLZ-BTED** dots in 4T1 tumor-bearing mice at 192 h under an 808 nm laser excitation (1000 nm LP, 100 ms, 90 mW cm^{-2}). (B) The *ex vivo* fluorescent signal of different organs and tumor tissues.

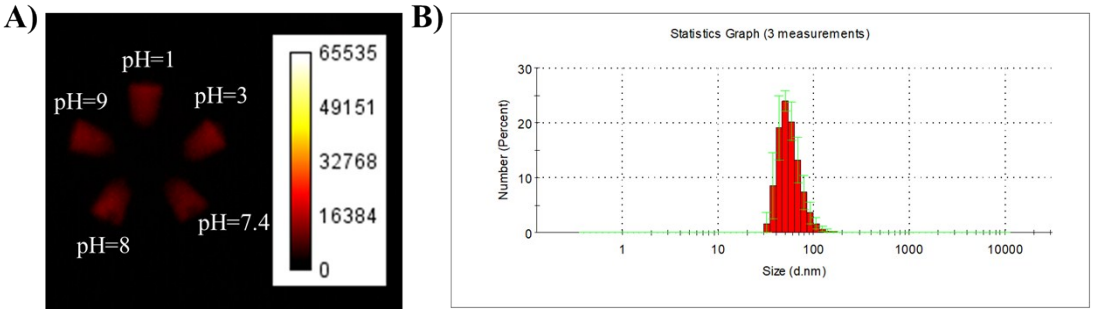

Figure S10. (A) NIR-II images (90 mW cm^{-2}, 808 nm excitation, 1000 nm LP and 10 ms) of **HLZ-BTED** dots (10 μg/mL) in PBS buffers of different pH values (pH1-pH9). (B) The hydrodynamic sizes (~60 nm) of **HLZ-BTED** dots in buffer with pH 1 based on DLS measurement (n = 3).

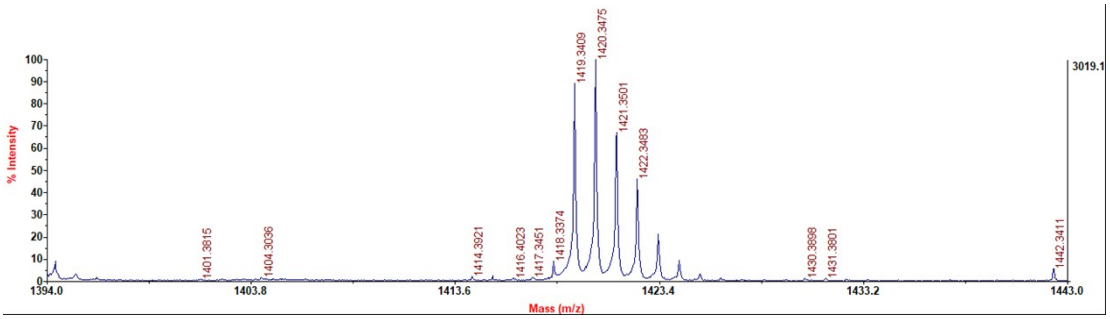

Figure S11. MALDI-TOF-MS Spectrum of **HLZ-BTED**

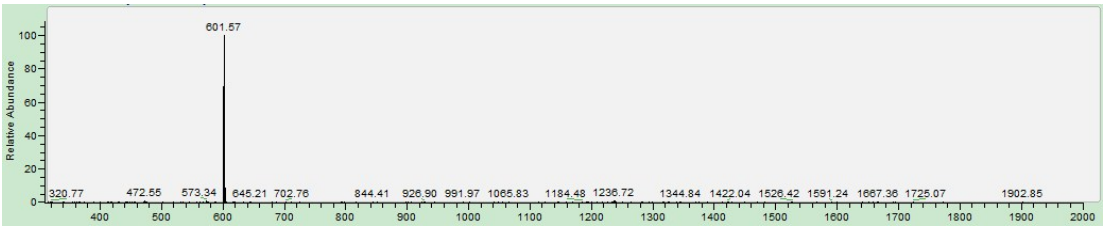

Figure S12. ESI-MS Spectrum of compound **3**

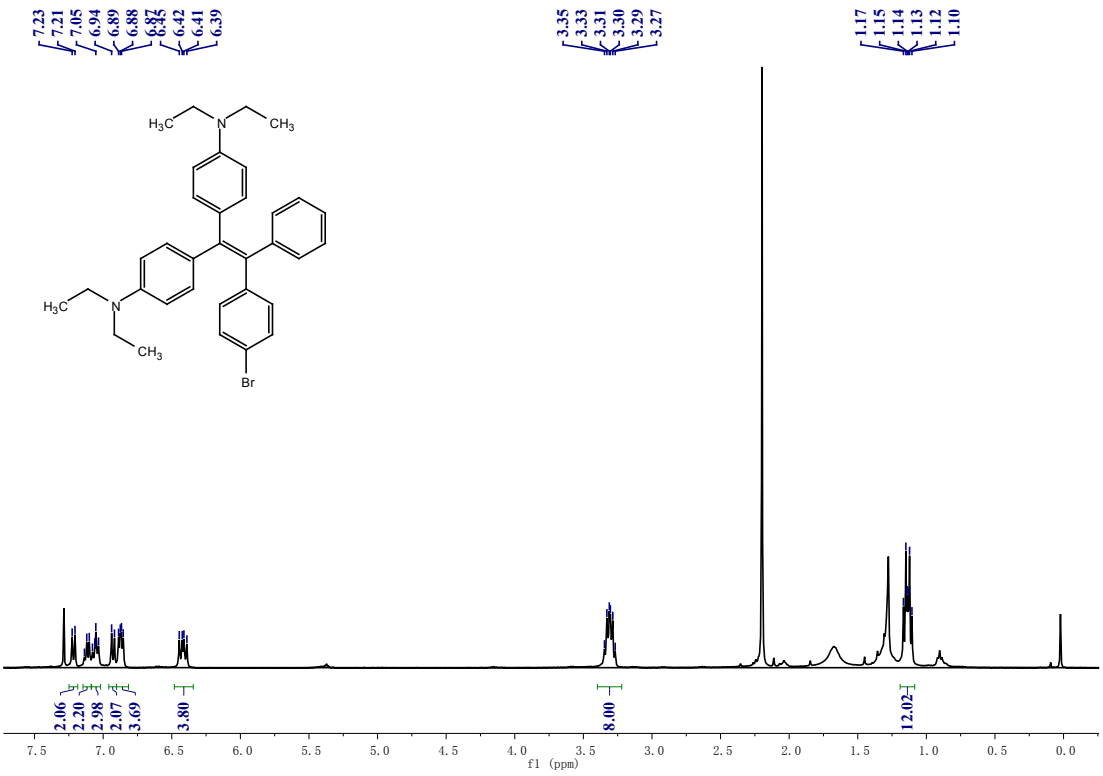

Figure S13. ^{1}H NMR for Compound **2**

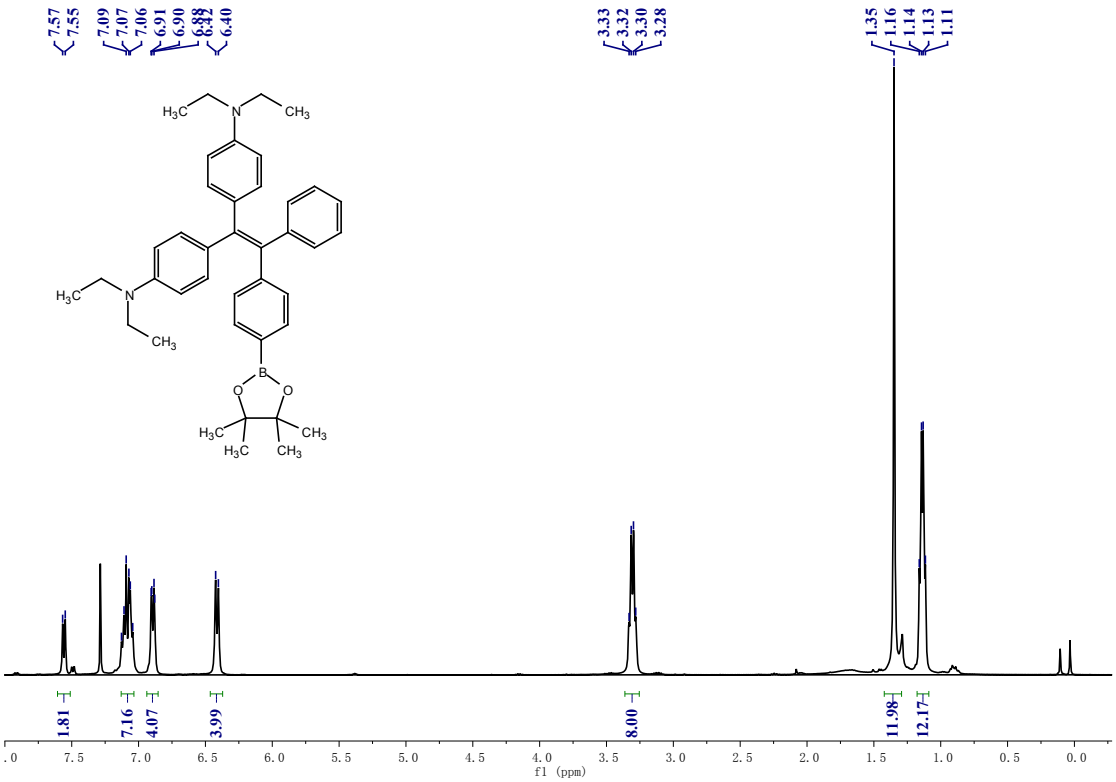

Figure S14.[1]H NMR for Compound **3**

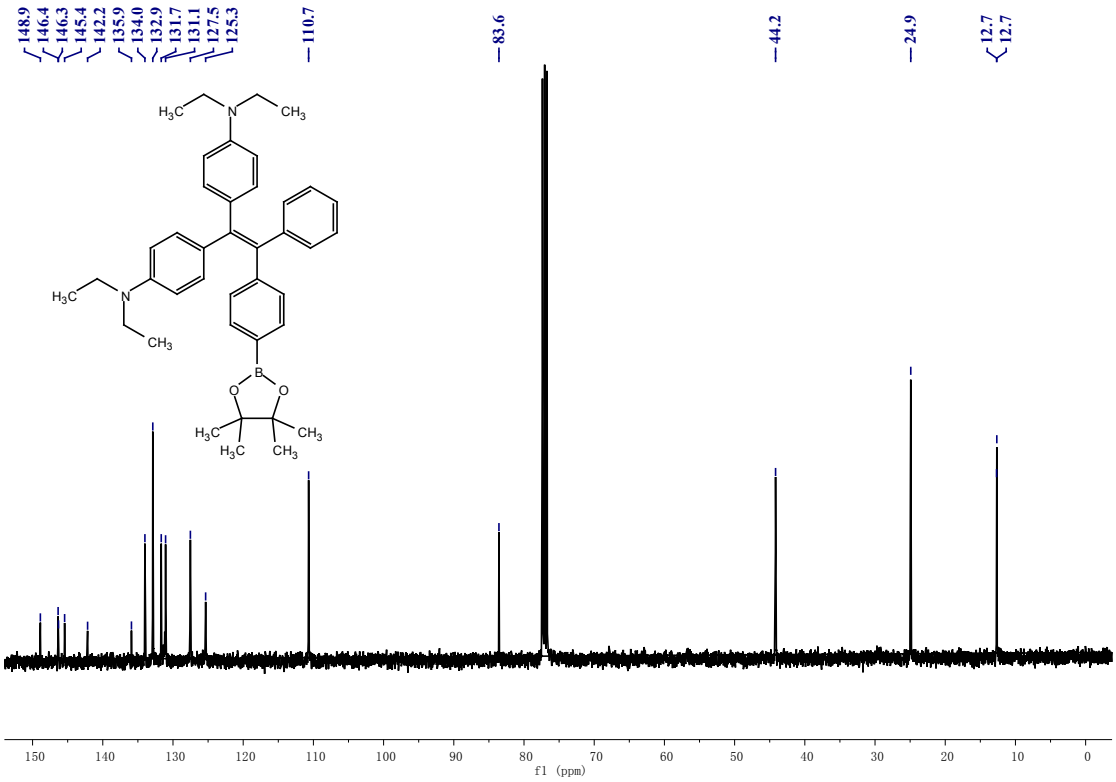

Figure S15. ^{13}C NMR for Compound **3**

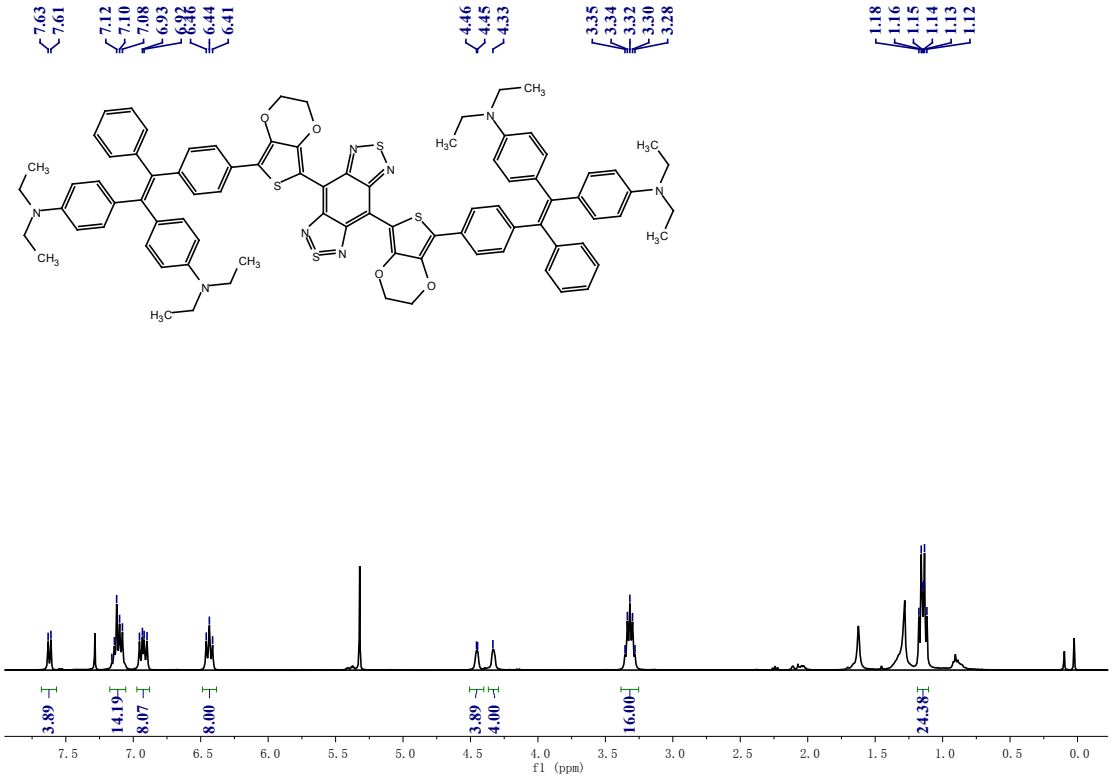

Figure S16. ^{1}H NMR for **HLZ-BTED**

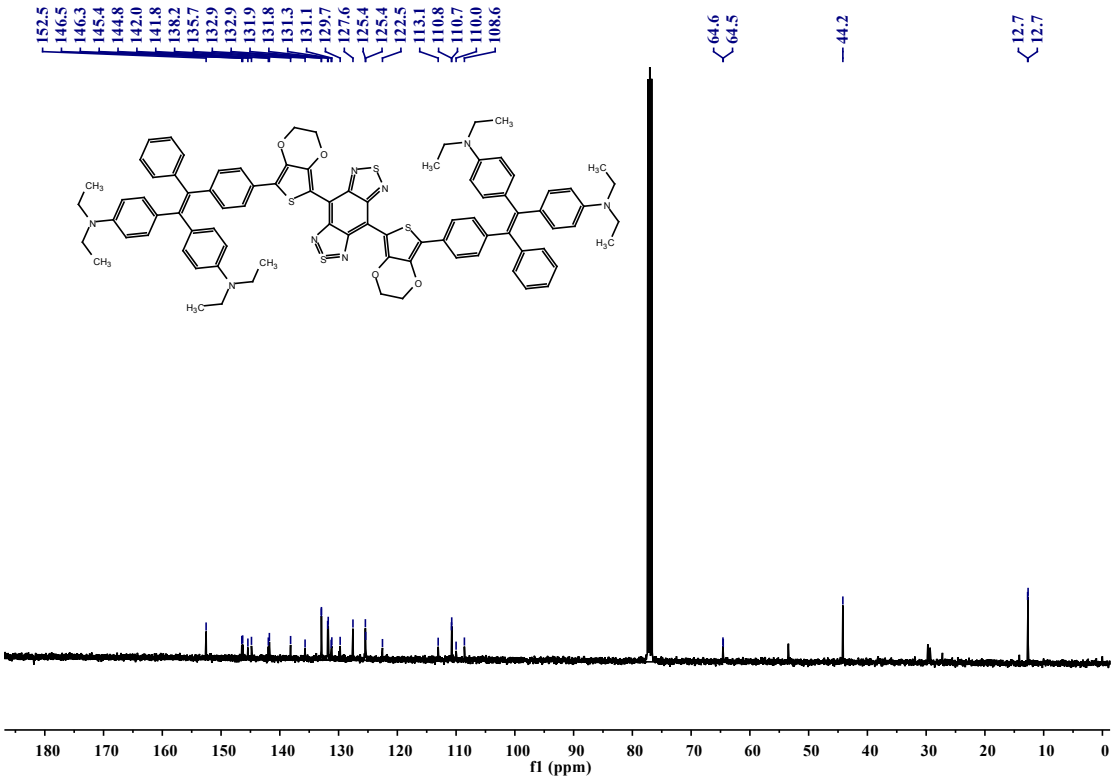

Figure S17. ^{13}C NMR for **HLZ-BTED**

Materials and General Experimental Methods.

NMR spectra were carried out with a Bruker AV400 magnetic resonance spectrometer. Chemical shifts (ppm) were reported relative to internal $CDCl_3$ (^1H, 7.26 ppm and ^{13}C, 77.0 ppm). MALDI-TOF-MS experiments were performed on an Applied Biosystems 4700 MALDI TOF mass spectrometer. UV-vis-NIR spectra were tested with a PerkinElmer Lambda 25 UV-Vis spectrophotometer. NIR fluorescence spectrum was recorded on an Applied NanoFluorescence spectrometer at room temperature with an excitation laser source of 785 nm. The NIR-II system was purchased from Suzhou NIR-Optics Technologies CO., Ltd. Hydrodynamic diameter and zeta potentials were measured using a Malvern Zetasizer Nano ZS. Transmission electron microscopy (TEM) images were recorded on a JEM-2100 TEM system at an accelerating voltage of 200 kV. Tetrahydrofuran (THF) was freshly distilled from sodium/benzophenone. DSPE-mPEG (5 kDa) was purchased from Ponsure Biotechnology CO., Ltd. All other standard synthesis reagents were purchased from commercial suppliers (such as Aldrich, Energy Chemical) and used without further purification unless otherwise noted. TLC analysis was performed on silica gel plates and column chromatography was conducted over silica gel (mesh 200-300), both of which were obtained from the Qingdao Ocean Chemicals. Compound **4** (4,7-bis(7-bromo-2,3-dihydrothieno[3,4-*b*][1,4]dioxin-5-yl)-5,6-dinitrobenzo[*c*][1,2,5]thiadiazole) was obtained according to previous report.[2]

Synthesis and characterization

Synthesis of compound 2[3]

To a solution of 4-bromobenzophenone (1.45g, 5.55 mmol) and 4,4'-Bis(diethylamino) benzophenone (1.5 g, 4.62 mmol) and Zinc powder (1.50g, 22.94 mmol) in freshly distilled THF (15 mL), $TiCl_4$ (18.75 mL, 18.75 mmol) was dropped into the reaction mixture at 0 °C under an argon atmosphere with rapid stirring over 30 min. The mixture was heated to 80 °C for 24 h. After being cooled to room temperature, the reaction was quenched by the addition of 50 mL 10% aq K_2CO_3; the mixture was filtered to remove insoluble materials and washed with dichloromethane. The organic layer was dried with anhydrous Na_2SO_4 and filtered. The solution was evaporated. The crude product was purified by column chromatography (PE:EA = 100:1) to give 0.72 g (1.30 mmol) of compound **2** as a light yellow solid in 28% yield. ^{1}H NMR (400 MHz, $CDCl_3$) δ (ppm): 7.20 (d, 2H), 7.07 (m, 5H), 6.88 (d, 6H), 6.42 (d, 4H), 3.30 (m, 8H), 1.13 (m, 12H).

Synthesis of compound 3

To a solution of compound **2** (280 mg, 0.51 mmol), bis(pinacolate)diboron (193 mg, 0.76 mmol) and KOAc (124 mg, 1.26 mmol) and in Dioxane (10 mL) was added bis(triphenylphosphine)palladium(II) dichloride (36 mg, 0.05 mmol) under an argon atmosphere. Then the reaction mixture was heated in an oil bath at 110 °C for 24 h. After the reaction mixture was cooled down to room temperature, the solvent was removed by evaporation. The residue was dissolved in dichloromethane and the resulting solution was washed with water, saturated aqueous brine and dried with anhydrous Na_2SO_4. The solution was evaporated. The crude product was purified by column chromatography (PE:EA = 20:1) to give 243 mg (0.40 mmol) of compound **3**

as a yellow solid in 80% yield. ^{1}H NMR (400 MHz, $CDCl_3$) δ (ppm): 7.53 (d, 2H), 7.05 (m, 7H), 6.87 (d, 4H), 6.39 (d, 4H), 3.28 (m, 8H), 1.32 (s, 12H), 1.11 (m, 12H). ^{13}C NMR (101 MHz, $CDCl_3$) δ 148.9, 146.4, 146.3, 145.4, 142.2, 135.9, 134.0, 132.9, 131.7, 131.1, 127.5, 125.3, 110.7, 83.6, 44.2, 24.9, 12.7. ESI-MS *m*/*z*: $[M+H]^+$ calcd for $C_{40}H_{49}BN_2O_2^+$, 601.4; found, 601.6.

Synthesis of compound 5

To a solution of compound **3** (388 mg, 0.65 mmol) and compound **4** (204 mg, 0.31 mmol) in THF (15 mL) was bubbled with argon for 5 min. Potassium carbonate (85mg, 0.62 mmol) in 2 mL distilled water and 1,1'-Bis(diphenylphosphino)ferrocenepalladium(II)dichloride dichloromethane complex (50 mg, 0.06 mmol) were added to the above reaction mixture under an argon atmosphere. The mixture was heated in an oil bath at 75 °C for 10 h. After cooling to room temperature, the solvent was removed in vacuo. The residue was dissolved in dichloromethane, and the resulting solution was washed with water, saturated aqueous brine. After drying over anhydrous sodium sulfate and removal of the solvents under reduced pressure, The crude product was purified by column chromatography (PE:DCM = 2:1) to give 334 mg (0.23 mmol) of compound **5** as a green solid in 75% yield. Compound **5** was utilized for the next step without characterization.

Synthesis of HLZ-BTED

Zinc powder (228 mg, 3.51 mmol) and NH_4Cl (99 mg, 2.11 mmol) were added to a stirred solution of compound **5** (85 mg, 0.06 mmol) in dichloromethane (8 mL) and 90% methanol (8 mL) under an argon atmosphere. After being stirred at room

temperature for 4 h, the solution was filtered through Celite pad, diluted with dichloromethane, and washed with water, saturated aqueous $NaHCO_3$, and saturated aqueous brine. The organic phase was dried over anhydrous Na_2SO_4, filtered and concentrated under vacuum to afford a yellow solid which was utilized for the next step without further purification.

To a dark yellow solution in anhydrous pyridine (4 mL) was added N-thionylaniline (0.40 mL, 3.51 mmol, 489 mg) and chlorotrimethylsilane (0.41 mL, 4.68 mmol, 508 mg). The mixture was heated in an oil bath at 80°C for 20 h. The reaction mixture was allowed to cool down to room temperature, poured into iced water, extracted with dichloromethane. The combined organic layer was washed with water, saturated aqueous brine, dried over anhydrous Na_2SO_4, and concentrated in vacuo. The residue was purified by flash column chromatography on silica gel (PE:DCM = 2:1) to yield the product **HLZ-BTED** as a dark green solid (42 mg, two step 51% yield). ^{1}H NMR (400 MHz, $CDCl_3$) δ (ppm): 7.60 (d, 4H), 7.08 (m, 14H), 6.90 (m, 8H), 6.40 (m, 8H), 4.43 (s, 4H), 4.31 (s, 4H), 3.29 (m, 16H), 1.11 (m, 24H). ^{13}C NMR (101 MHz, $CDCl_3$) δ 152.5, 146.5, 146.3, 145.4, 144.8, 142.0, 141.8, 138.2, 135.7, 132.9, 131.9, 131.8, 131.3, 131.1, 129.7, 127.6, 125.4, 122.5, 113.1, 110.8, 110.7, 110.0, 108.6, 64.6, 64.5, 44.2, 12.7. MALDI-TOF-MS *m/z*: $[M+H]^+$ calcd for $C_{86}H_{83}N_8O_4S_4^+$, 1419.5420; found, 1419.3409.

Fabrication of HLZ-BTED dots

The **HLZ-BTED** was dissolved in THF at a concentration of 1 mg/mL and quickly injected into an aqueous solution of DSPE-mPEG (5 kDa) at a concentration of 1

mg/mL with 1 : 6 volume ratio with an ice bath under continuous sonication. A microtip probe sonicator (Fisher Scientific model FB505) was applied to disperse organic components vigorously in water for 6 minutes. After THF was removed by nitrogen flow, this reaction mixture was centrifuged at 12,000 rpm for 10 min using 50 kDa molecular weight cut-off filter to remove unreacted reagents, and washed by water 6 times using the same filter. The complex was finally re-dissolved in 1 mL water. The amount of **HLZ-BTED** encapsulated in the nanoparticles was measured by UV-vis-NIR spectrophotometer at 874 nm.

Determination of the optical spectrum and fluorescence quantum yield.

The fluorescence quantum yield measurement was carried out using IR-26 whose quantum yield has been reported as 0.5% in 1,2-dichloroethane (DCE) as reference. In a typical procedure, a series of solutions of IR-26 in DCE with absorbance values at 785 nm to be ~ 0.10, ~ 0.08, ~ 0.06, ~0.04 and ~0.02 were prepared respectively. Optical absorbance spectra of the five solutions were measured using PerkinElmer Lambda 25 UV-Vis spectrophotometer. NIR emission spectra of the five solutions with linearly spaced concentrations were measured using Applied NanoFluorescence spectrometer. The 785 nm laser was used as the excitation source and a 900 nm longpass filter was used as the emission filter to acquire the emission spectrum in the range of 916 to 1500 nm. Same solution preparation, absorbance and fluorescence spectra measurements were performed for **HLZ-BTED** and **HLZ-BTED** dots.

Cell Line and Animal Model.

Mouse mammary tumor cell line 4T1 and mouse fibroblastic cell line L929 were purchased from the China Center for Type Culture Collection (CCTCC). All cells were grown in a humidified atmosphere at 37 °C with 5% CO_2 atmosphere. 4T1 Cells were cultured in Dulbecco's Modified Eagle Medium (DMEM, Gibco), and L929 cells were maintained in Mimumum Essentiul Medium (MEM, Gibco), supplemented with 10% fetal bovine serum, 100 IU mL^{-1} penicillin, 100 μg mL^{-1} streptomycin. For 4T1 breast tumor model establishment, 4T1 cells (roughly 2×10^6 in 75 μL of DMEM medium) were subcutaneously injected into the right leg of the 6-week-old female BALB/c nude mice which are purchased from the Center for Disease Prevention and Control in Hubei Province, China. The tumors were allowed to reach ~60 mm^3 for small animal fluorescent imaging studies.

Blood Circulation.

To investigate the pharmacokinetics of **HLZ-BTED** dots, the AIE dots was intravenously injected into KM female mice (n = 3). Blood samples were collected at pre-injection, 5, 10, 20, 30, 60, 180, 360, 540, 720, 1,440, 2,880 min post-injection, respectively. Then, the samples were imaged under the NIR-II fluorescence imaging system, followed by the fluorescent intensity analysis (deducting blank blood fluorescence values) of different time points images using ImageJ software (ImageJ 1.51j8, National Institutes of Health, USA). The time-dependent relative fluorescent

intensity in blood were fitted with a first-order exponential decay to evaluate the blood half-life.

In Vitro Cytotoxicity and Cellular Uptake Studies.

The cytotoxicity was investigated by a standard MTT assay. The cytotoxicities of **HLZ-BTED** dots were obtained by measuring the cell viability of normal cells L929 and tumor cells 4T1 using the MTT assay. The L929, and 4T1 cells were seeded in a 96-well plate (2000 cells per well). After 12 h, the medium was substituted with the fresh medium contained **HLZ-BTED** dots with different concentrations. Followed by incubation for 24 h, then a standard MTT method was performed for measuring the cell viability. For in vitro cellular uptake experiment, the 4T1 cells were seeded in a 6-well plate ($1.5*10^4$ cells per well). After 12 h, the medium was substituted with the fresh medium contained **HLZ-BTED** dots (100 μg/mL). Followed by incubation for 3 hours or 24 hours, 4T1 cells were treated with trypsin to obtain cell suspension. The cells were washed twice with PBS and then resuspended in PBS for NIR-II imaging.

In Vivo Toxicity Studies.

For the evaluation of the in vivo toxicity of **HLZ-BTED** dots, the healthy KM mice purchased from the Center for Disease Prevention and Control in Hubei Province were intravenously injected via the tail vein with PBS (0.2 mL), **HLZ-BTED** dots (0.2 mL, 7.5 mg kg^{-1}or 15 mg kg^{-1}), n = 3 per group. The body weight of these mice were recorded and the mice were sacrificed after 31 d post-injection. The major organs, liver,

lung, heart, spleen, and kidneys were excised for fixing with 10 % buffered formalin. Tissue samples were stained with hematoxylin and eosin (H&E) and subsequently imaged using a digital microscope.

In Vivo NIR-II Fluorescence Imaging.

All NIR-II fluorescent images were collected using a NIR-II imaging system with the indium-gallium-arsenide (InGaAs) camera (Princeton Instruments) which was purchased from Suzhou NIR-Optics Technologies CO., Ltd. The excitation light source was an 808 nm diode laser. The laser power density was 90 mW cm^{-2} with a 1,000 nm long-pass filter and 180 mW cm^{-2} with a 1,250 nm long-pass filter during *in vivo* imaging. The mice were anesthesized by intraperitoneal injection of pentobarbital sodium solution (50 mg kg^{-1}) during injection and NIR-II imaging. For tumor and tumor-feeding blood vessels imaging, the BALB/c mice bearing subcutaneous 4T1 tumors were given **HLZ-BTED** dots (0.2 mL, 10 mg kg^{-1}) via tail vein injection. After injection, the mice were mounted in the prone position beneath the laser for imaging at various time points. For hind limb vasculature and incomplete hind limb ischemia imaging, **HLZ-BTED** dots (0.2 mL, 15 mg kg^{-1}) were injected into C57BL/6 mice via the tail vein. And animals were mounted in the supine position for imaging. For gastrointestinal tract imaging, BALB/c mice in health or in intestinal obstruction were gavaged with **HLZ-BTED** dots (0.1 mL, 5 mg kg^{-1}). After gavage, the mice were mounted in the supine position and the abdomens were visualized at various time

points. At the same time, the NIR-II images and movies of gastrointestinal tract in health and in disease were collected by NIR-II imaging system.

Ex Vivo Biodistribution Analysis.

For tumor imaging, at 192 h after injection of **HLZ-BTED** dots into 4T1 tumor-bearing BALB/c mice, mice (n = 3) were sacrificed, then the major organs and tumor tissues were collected for imaging study. For gastrointestinal tract imaging, the healthy mice (n = 3) and intestinal obstruction mice (n = 3) were sacrificed at 24 h after gavaged with **HLZ-BTED** dots. The gastrointestinal tract was excised for imaging. *Ex vivo* organs and tumor tissues or gastrointestinal tract were imaged in the NIR-II imaging system which used for *in vivo* fluorescent imaging, and the laser power density was 90 mW cm^{-2}.

Reference

[1] Gaussian 09, Revision A.1, M. J. Frisch, G. W. Trucks, H. B. Schlegel, G. E. Scuseria, M. A. Robb, J. R. Cheeseman, G. Scalmani, V. Barone, B. Mennucci, G. A. Petersson, H. Nakatsuji, M. Caricato, X. Li, H. P. Hratchian, A. F. Izmaylov, J. Bloino, G. Zheng, J. L. Sonnenberg, M. Hada, M. Ehara, K. Toyota, R. Fukuda, J. Hasegawa, M. Ishida, T. Nakajima, Y. Honda, O. Kitao, H. Nakai, T. Vreven, J. A. Montgomery, Jr., J. E. Peralta, F. Ogliaro, M. Bearpark, J. J. Heyd, E. Brothers, K. N. Kudin, V. N. Staroverov, R. Kobayashi, J. Normand, K. Raghavachari, A. Rendell, J. C. Burant, S. S. Iyengar, J. Tomasi, M. Cossi, N. Rega, J. M. Millam, M. Klene, J. E. Knox, J. B. Cross, V. Bakken, C. Adamo, J. Jaramillo, R. Gomperts, R. E. Stratmann, O. Yazyev, A. J. Austin, R. Cammi, C. Pomelli, J. W. Ochterski, R. L. Martin, K. Morokuma, V. G. Zakrzewski, G. A. Voth, P. Salvador, J. J. Dannenberg, S. Dapprich, A. D. Daniels, O. Farkas, J. B. Foresman, J. V. Ortiz, J. Cioslowski, and D. J. Fox, Gaussian, Inc., Wallingford CT, **2009**.

[2] X. Zeng, Y. Xiao, J. Lin, S. Li, H. Zhou, J. Nong, G. Xu, H. Wang, F. Xu, J. Wu, Z. Deng, X. Hong, *Adv. Healthcare Mater.* **2018**, 1800589.

[3] X. Y. Shen, Y. J. Wang, E. Zhao, W. Z. Yuan, Y. Liu, P. Lu, A. Qin, Y. Ma, J. Z. Sun, B. Z. Tang, *J. Phys. Chem. C* **2013**, 117, 7334.